Surface Geosciences

Quantitative evaluation of soil processes using in situ-produced cosmogenic nuclides

Erik Thorson Brown [a,*], Fabrice Colin [b], Didier L. Bourlès [c]

[a] *Large Lakes Observatory, University of Minnesota, Duluth, MN 55812, USA*
[b] *IRD/UM-GECO; CEREGE, Europole de l'Arbois, 13545 Aix-en-Provence cedex 04, France*
[c] *CEREGE, Europole de l'Arbois, 13545 Aix-en-Provence cedex 04, France*

Abstract

In situ-produced cosmogenic nuclides provide a means for quantitative evaluation of a wide range of weathering and sediment transport processes. Although these nuclides have received attention for their power as geochronometers of surface exposure, it may be argued that they are more broadly suited for study of surface processes. In many environments, they may be used to evaluate collapse, erosion, burial, bioturbation, and creep, as well as providing a qualitative basis for distinguishing allochthonous from autochthonous materials. In addition, these nuclides can provide quantitative information on rates of erosion on scales of landforms and drainage basins. Here, we review the systematics of cosmogenic nuclide production within the Earth's surface, and present field examples demonstrating the utilization of in situ-produced cosmogenic nuclides distributions for evaluation of a range of soil evolution processes. ***To cite this article: E.T. Brown et al., C. R. Geoscience 335 (2003).***
© 2003 Académie des sciences. Published by Elsevier SAS. All rights reserved.

Résumé

Évaluation quantitative des mécanismes pédologiques utilisant les nucléides cosmogéniques produits in situ. Les nucléides produits in situ constituent un moyen d'évaluation d'une large palette de mécanismes d'altération et de transport sédimentaire. Bien que ces nucléides aient été l'objet d'une attention particulière, en raison de leur pouvoir de géochronomètres de l'exposition de surface, il peut être plaidé qu'ils conviennent plus largement pour l'étude des processus de surface. Dans de nombreux environnements, ils peuvent être utilisés pour évaluer l'affaissement, l'érosion, l'enfouissement, la bioturbation et le fluage, aussi bien que pour fournir une base qualitative de distinction entre matériaux allochtones et autochtones. En outre, ces nucléides peuvent apporter une information quantitative sur les taux d'érosion à l'échelle de paysages ou de bassins hydrographiques. Ici sont présentés une revue de la systématique de production des nucléides cosmogéniques à la surface de la Terre et des exemples de terrain démontrant l'utilisation de la répartition des nucléides cosmogéniques produits in situ pour l'évaluation d'un ensemble de processus d'évolution des sols. ***Pour citer cet article : E.T. Brown et al., C. R. Geoscience 335 (2003).***
© 2003 Académie des sciences. Published by Elsevier SAS. All rights reserved.

---

* Corresponding author.
 E-mail address: etbrown@d.umn.edu (E.T. Brown).

1. Introduction

Cosmic radiation present at ground level produces cosmogenic nuclides (including ^{3}He, ^{10}Be, ^{14}C, ^{21}Ne, ^{26}Al and ^{36}Cl) within mineral lattices of exposed rock. Their production rates vary with location; cosmic rays are attenuated as they penetrate the atmosphere and deflected by the Earth's magnetic field so production rates are lower at low elevation and low latitudes. In addition, production rates have varied in the past in response to changes in the geomagnetic field strength. In surface rocks, the production rates of most cosmogenic nuclides decrease exponentially with depth, so production is limited essentially to the upper few meters of an exposed rock surface. These in situ produced cosmogenic nuclides are thus useful for dating periods of surface exposure (see reviews in [12,19, 31]). Accumulation of cosmogenic nuclides can thus be used to date geological events that exhume material from depth (e.g., glaciation, mass wasting, volcanic activity, and meteor impact). However, once a steady-state balance is reached between production and losses (due to radioactive decay or to erosion of a rock's surface) concentrations and distributions of these nuclides no longer yield geochronological information. At this point they provide both qualitative and quantitative information on physical processes of soil development.

2. Systematics of in situ production of cosmogenic nuclides

Use of cosmogenic nuclides for examination of surficial processes requires a detailed understanding of the production systematics of these nuclides, in particular the variability of their production as a function of subsurface depth. The nuclides most commonly used for studies of surficial environments include ^{10}Be, ^{26}Al and ^{36}Cl (half-lives of 1.5, 0.70 and 0.30 Myr, respectively). Our work has focused on ^{10}Be produced in quartz. Quartz is abundant, easily purified, and easily dissolved for ^{10}Be extraction. In addition, the production mechanisms of ^{10}Be in quartz are simple and well described, making its distributions more readily interpretable.

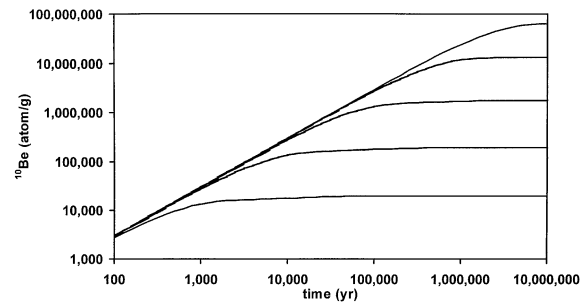Beryllium-10 is produced by nuclear reactions induced by three classes of cosmic radiation: neutrons,

Fig. 1. Accumulation of ^{10}Be as a function of surface exposure time and erosion rate. From top to bottom, the curves represent constant erosion rates of 0, 1, 10, 100 and 1000 mm kyr^{-1}. For the case of no erosion, the ^{10}Be concentration increases over time approaching a steady-state balance between production and losses by radioactive decay. At higher rates of erosion, ^{10}Be concentrations reach steady state more rapidly and at lower concentrations. Steady-state concentrations provide only lower limits to the duration of surface exposure.

Fig. 1. Accumulation de ^{10}Be en fonction du temps d'exposition de surface et du taux d'érosion. Du haut vers le bas, les courbes représentent des taux constants d'érosion de 0, 1, 10, et 1000 mm ka^{-1}. Dans le cas d'une absence d'érosion, la concentration en ^{10}Be augmente avec le temps en approchant un bilan d'équilibre entre production et pertes par désintégration radioactive. Pour de forts taux d'érosion, les concentrations en ^{10}Be atteignent un état d'équilibre plus rapidement et à de plus faibles concentrations. Les concentrations, à l'équilibre, ne fournissent que des limites inférieures à la durée d'exposition de surface.

stopping muons, and fast muons [16,17]. These particles are attenuated as they penetrate into matter, so the production of cosmogenic nuclides may be represented by a combination of exponentials that decrease with depth into rock. As ^{10}Be is essentially immobile after production, its concentration in surficial rock, N (at g^{-1}), can be related to the rock's history of near-surface exposure through Eq. (1):

$$N(t) = \frac{P_n}{(\varepsilon L_n^{-1} + \lambda)}\left[1 - e^{-t(\varepsilon L_n^{-1} + \lambda)}\right]$$
$$+ \frac{P_{\mu\text{stop}}}{(\varepsilon L_{\mu\text{stop}}^{-1} + \lambda)}\left[1 - e^{-t(\varepsilon L_{\mu\text{stop}}^{-1} + \lambda)}\right]$$
$$+ \frac{P_{\mu\text{fast}}}{(\varepsilon L_{\mu\text{fast}}^{-1} + \lambda)}\left[1 - e^{-t(\varepsilon L_{\mu\text{fast}}^{-1} + \lambda)}\right] \qquad (1)$$

Here, P_n, $P_{\mu\text{stop}}$, and $P_{\mu\text{fast}}$ represent the production rates (at g^{-1} yr^{-1}) for each of the three mechanisms normalized for altitude and geomagnetic latitude, ε is the erosion rate (g cm^{-2} yr^{-1}), L_n, $L_{\mu\text{stop}}$, and $L_{\mu\text{fast}}$ are, respectively, the effective attenuation lengths of
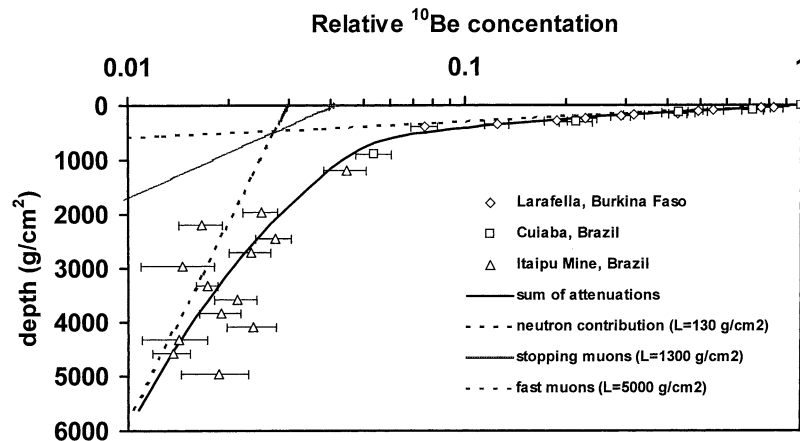
Relative ^{10}Be concentration

Fig. 2. Depth profile of ^{10}Be produced by neutrons, stopping muons, and fast muons, with data from outcropping quartz veins in Burkina Faso and Brazil [3,6]. Curves were calculated as described in the text using these field results in combination with experimental data [16,17]. An erosion rate of 1.9 m Myr^{-1}, which yields the observed steady-state surface concentration, was employed. At greater depths, the role of muons becomes increasingly apparent.

Fig. 2. Profil en fonction de la profondeur du ^{10}Be produit par des neutrons, des muons à l'arrêt et des muons rapides, avec les données obtenues sur des affleurements de veines de quartz au Burkina Faso et au Brésil [3,6]. Les courbes ont été calculées comme décrit dans le texte, en utilisant les résultats de terrain combinés aux données expérimentales [16,17]. Un taux d'érosion de 1,9 m Ma^{-1}, qui produit la concentration de surface à l'état d'équilibre observé, a été utilisé. Aux plus grandes profondeurs, le rôle des muons devient plus nettement apparent.

cosmic ray neutrons, stopping muons and fast muons, t is the time since initiation of surface exposure and λ is the radioactive decay constant (yr^{-1}). Depths in soil or rock as well as attenuation lengths are typically expressed in terms of mass per unit area to account for variation in material density. Cosmogenic nuclide concentrations in a rock surface increase with time (allowing their use as a geochronometer of surface exposure) until they reach a steady state, where production is balanced by losses by erosion and by radioactive decay (Fig. 1).

Laboratory- and field-based approaches have been employed to investigate the systematics of cosmogenic nuclide production. Recent laboratory studies involving bombardment of targets by high-energy neutrons, fast muons and stopping muons have provided information on the production of cosmogenic nuclides [16, 17]. In combination with measured depth profiles of ^{10}Be in exposed bedrock in tectonically stable environments [3,6,9], these are providing the quantitative description of ^{10}Be production as a function of depth into rock needed as a basis for rigorous application of this approach. These results indicate that neutrons, stopping muons and fast muons account for approximately 98.2, 1.2 and 0.6% of production at the surface,

respectively. Depth variability by the three mechanisms can be described as exponential attenuation with e-folding lengths corresponding to approximately 130, 1300 and 5000 g cm^{-2}, respectively (Fig. 2). These results have identified the role of production induced by fast muons at depth, which must be taken into account when evaluating data from soil or rock profiles deeper than 1–2 m. This review applies these new values to a range of approaches used in evaluation of soil development and sediment transport.

3. Applications for evaluation of physical perturbation to rock and soil profiles

Depth profiles of cosmogenic nuclide in soils are uniquely suited for study of a range of processes that generate and destroy soils at geomorphic surfaces. The basic strategy evaluates such processes (e.g., erosion, collapse, burial, bioturbation, soil creep) by examining perturbation of measured depth profiles of cosmogenic nuclide concentrations relative to theoretical profiles expected for a simple undisturbed system. The following sections discuss the effects of each of these physical processes on cosmogenic nuclide accumulation.
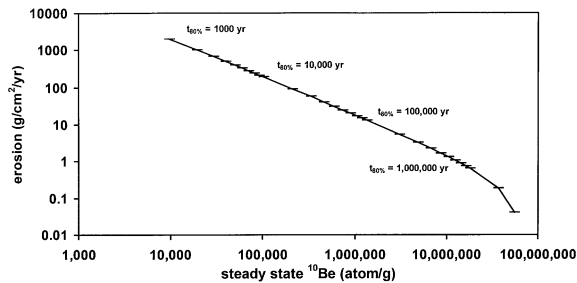
Fig. 3. Relationship between steady-state ^{10}Be concentration and average erosion rate. The tick marks represent the time required to achieve 80% of the steady-state concentration, and thus provide an indication of the time period represented by an erosion rate calculated from steady-state ^{10}Be.

Fig. 3. Relation entre concentration en ^{10}Be à l'équilibre et taux d'érosion moyen. Les marques représentent le temps requis pour obtenir 80% de la concentration à l'équilibre et ceci fournit une indication sur la période de temps représentée par un taux d'érosion calculé à partir de l'état d'équilibre du ^{10}Be.

3.1. Erosion

Consider an unrealistic case in which erosion is the only physical process affecting a soil profile; the systematics of cosmogenic nuclide accumulation in such a profile will be identical to that of a profile through exposed bedrock. When independent evidence indicates that a surface has been exposed for sufficient time for the concentration of a cosmogenic nuclide to attain a steady state (such that production is balanced by losses through radioactive decay and erosion) the surface concentration may be used to quantify an average erosion rate (Fig. 1; Eq. (1) for $t \rightarrow \infty$). The time required to attain steady state depends on the erosion rate; hence the period time represented by the average erosion rate also varies with erosion rate (Fig. 3).

The form of a depth profile is also dependent upon erosion rates. At higher erosion rates, a particular bit of rock spends less time in the near-surface zone, leading to a smaller contribution of neutron-produced nuclides. As a consequence, the overall apparent production attenuation length will increase in surfaces undergoing erosion at greater rates. This contrasts with the apparent decrease in cosmic ray attenuation length induced by the processes discussed in the following sections. Variation in depth profiles induced by erosion is subtle compared to the variability of steady-state surface concentrations under differing erosion rates. Nev-
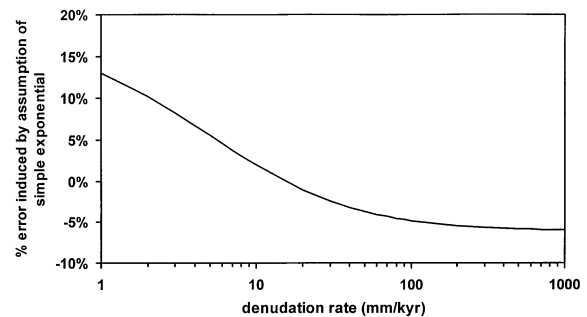

Fig. 4. Error induced in calculated erosion rated due to the assumption of a simple exponential decrease in production rate. Steady-state concentrations were calculated for a range of erosion rates using Eq. (1). Erosion rates were then calculated from these concentrations under the assumption of simple exponential attenuation of ^{10}Be production with an attenuation length of $155\ \mathrm{g\,cm^{-2}}$, and then compared to the rates employed in the original calculation.

Fig. 4. Erreur induite dans le calcul du taux d'érosion, due au fait que l'on admet une simple diminution exponentielle dans le taux de production. Les concentrations à l'équilibre ont été calculées pour une fourchette de taux d'érosion utilisant l'Éq. (1). Les taux d'érosion ont alors été calculés à partir de ces concentrations, en admettant une simple atténuation exponentielle de la production de ^{10}Be avec une longueur d'atténuation de $155\ \mathrm{g\,cm^{-2}}$, et ont ensuite été comparés à ceux utilisés dans le calcul initial.

ertheless, it needs to be considered when evaluating the effects of other processes on deep soil profiles.

When estimating erosion rates from surface concentrations, a single exponential with an attenuation length of $155\ \mathrm{g\,cm^{-2}}$ is a reasonable approximation for combined production by the three mechanisms. This may be illustrated through a simple model calculation that compares erosion rates determined from rock surface concentrations under the assumption of a simple exponential decrease in production rate with rates determined with consideration of the three exponentials. This calculation indicates that this simplifying assumption induces relatively small ($< 13\%$) errors. In the range of erosion rates typical for most regions on earth (5 to 100 $\mathrm{mm\,kyr^{-1}}$), these errors are less than $\sim 5\%$ (Fig. 4).

This approach can be used to determine landscape scale erosion rates if field evidence suggests that erosion of a sampled outcropping bedrock surface is representative of a wider area. Several studies have thus applied this technique to determine denudation rates for stable cratons with flat topography in a broad range of climate, at sites including the plateau of Mount

Roraima, Venezuela [7], southern Sahel of Burkina Faso [3,10], Brazilian tropical forest and savannah [4], Gabon [5], Namibian desert and highlands [1] and Kansas and Missouri, USA (E. Brown, unpublished results). The resultant rates all fall in the range of 3 to 8 m Myr^{-1}. This implies that, on the 10^5-year timescales recorded by cosmogenic nuclides for this low range of erosion rates, climate does not exert strong control on denudation rates.

3.2. Collapse

Soil columns are frequently perturbed by collapse – loss of mass from within a soil profile through chemical alteration and loss of volume due to decreased mechanical strength. Collapse has been evaluated under the assumption that elements such as Zr (or Ti) are immobile during chemical weathering and hence have concentrations that increase over time in a given soil [13]. The possibility of mobility of Zr during

weathering makes such estimates lower limits on collapse. Comparison of a depth profile of ^{10}Be from a site that has undergone significant collapse with a theoretical profile provides a means, independent of these assumptions of elemental immobility, for examining extent and timing of collapse (Fig. 5). If collapse occurs after most of the ^{10}Be has accumulated, ^{10}Be profiles are compacted by collapse, and the apparent attenuation length of ^{10}Be production is reduced relative to that of an undisturbed system. This apparent decrease in attenuation length contrasts with the apparent increased attenuation lengths associated with erosion. In soil profiles affected by both processes, erosion rates can be evaluated using surface concentrations, and collapse can be constrained by examining deviation from the profile expected for that erosion rate.

This approach is illustrated by a study of soil development at a site near the village of Malemba in the Republic of the Congo—Brazzaville (4°20′S, 12°25′E, 300 m) [3,9] (Fig. 5). At this site, quartz blocks (relicts
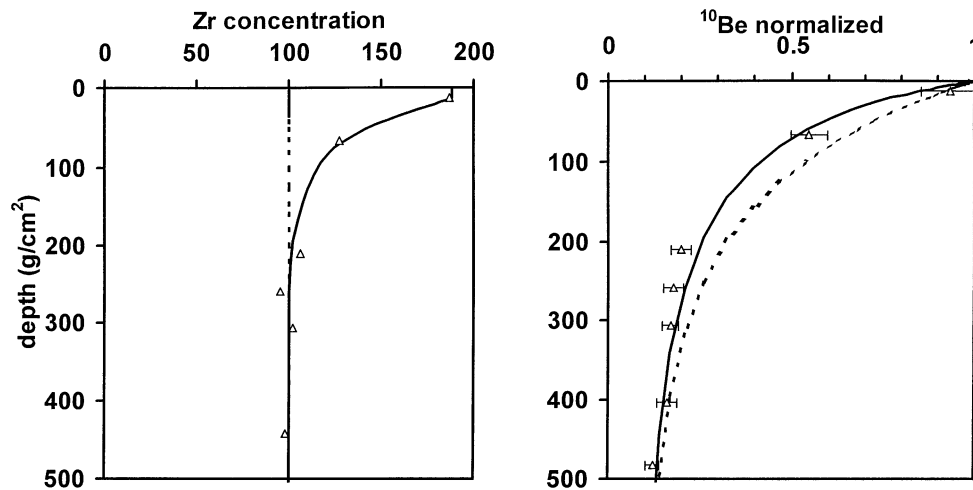

Fig. 5. Comparison of depth profiles of Zr and ^{10}Be in pre-collapse (dotted line) and post-collapse (solid lines) conditions at the Malemba Hill (Republic of the Congo) [9]. Collapse was calculated under the assumption of Zr immobility during chemical weathering by comparing Zr levels in the deep saprolite with profile samples. The pre-collapse ^{10}Be profile was calculated for an erosion rate of 12 m Myr^{-1}, which yields a steady-state surface concentration comparable to that observed at this site and in nearby ridge crest soils. In the post-collapse ^{10}Be profile sampling depths were adjusted using Zr-based mass loss. The coherence between the collapse indicated by Zr and ^{10}Be shows that collapse occurred after accumulation of the bulk of the ^{10}Be present in the soil.

Fig. 5. Comparaison des profils en fonction de la profondeur de Zr et ^{10}Be dans des conditions de pré-affaissement (ligne en pointillé) et post-affaissement (lignes continues) sur la colline de Malemba Hill (république du Congo) [9]. L'affaissement a été calculé en admettant l'immobilité de Zr pendant l'altération chimique par comparaison entre les teneurs en Zr de la saprolite profonde et les échantillons du profil. La courbe de pré-affaissement a été calculée pour un taux d'érosion de 12 m Ma^{-1}, ce qui fournit une concentration de surface à l'équilibre comparable à celle qui a été observée sur ce site et dans des sols d'une arête, au voisinage. Pour la courbe de post-affaissement du ^{10}Be, les profondeurs d'échantillonnage ont été ajustées en utilisant la perte massique basée sur Zr. La cohérence entre l'affaissement indiqué par Zr et par ^{10}Be montre que l'affaissement s'est produit après l'accumulation du total du ^{10}Be présent dans le sol.

of a subvertical quartz vein) penetrate through saprolite derived from weathering of Proterozoic schist and soil to outcrop at the summit of a small rounded hill. Measured distributions of ^{10}Be in the quartz blocks show a more rapid decrease in concentration with depth that would be expected for simple exposure and erosion. This reduction in apparent attenuation length is consistent with the collapse calculated under the assumption of Zr immobility, supporting the assumptions implicit in both calculations. Furthermore, as Zr-based estimates of collapse can integrate over longer periods than ^{10}Be-based estimates, the coherence of the results suggest that mass loss occurred relatively recently during the soil's history.

3.3. Burial

Depth profiles of cosmogenic nuclides can provide criteria for understanding whether material has undergone episodic exposure and burial. In static and eroding surfaces, concentrations decrease exponentially with subsurface depth. However, in a surface where material is being deposited, cosmogenic nuclide concentrations will not follow this simple exponential trend [5,8,20]. Accumulation and decay of a cosmogenic radionuclide may be described by Eq. (2):

$$
\begin{aligned}
N(t_B) &= \frac{P_n}{(-BL_n^{-1} + \lambda)} \\
&\quad \times e^{(-t_B BL_n^{-1})}\left[1 - e^{-t_B(-BL_n^{-1}+\lambda)}\right] \\
&\quad + \frac{P_{\mu stop}}{(-BL_{\mu stop}^{-1} + \lambda)} \\
&\quad \times e^{(-t_B BL_{\mu stop}^{-1})}\left[1 - e^{-t_B(-BL_{\mu stop}^{-1}+\lambda)}\right] \\
&\quad + \frac{P_{\mu fast}}{(-BL_{\mu fast}^{-1} + \lambda)} \\
&\quad \times e^{(-t_B BL_{\mu fast}^{-1})}\left[1 - e^{-t_B(-BL_{\mu fast}^{-1}+\lambda)}\right] \\
&\quad + N(0)\, e^{(-\lambda t_B)}
\end{aligned}
\tag{2}
$$

Here B represents a rate of burial (g cm^{-2} yr^{-1}), t_B represents burial time and $N(0)$ represents the concentration of the cosmogenic radionuclide at the time of burial. Note that this expression follows a particular bit of rock or soil as it is buried, in contrast to Eq. (1), which describes the concentration at the eroding surface. In general, surfaces undergoing burial will show

a subsurface maximum. The exact form of the profile depends on cosmogenic nuclide concentrations of the material being buried, as well as the burial rate. Nevertheless, the profiles can be employed to identify profiles where burial is occurring.

Quantitative information on burial of previously exposed rock may be obtained from ratios of cosmogenic radionuclides with differing half-lives (for example, ^{26}Al:^{10}Be, with $t_{1/2}$ of 0.7 and 1.5×10^6 yr, respectively). In exposed rock, this ratio is dependent on relative production rates of these nuclides, time of exposure, and losses by erosion and by radioactive decay. The ratio ^{26}Al:^{10}Be has a narrow range of possible values (2.8–6.0), which is even more limited (4.8–6.0) in rock surfaces eroding at rates greater than 5 mm kyr^{-1}. However, if material is buried after an episode of surface exposure, radioactive decay can decrease this ratio well below the range observed at the surface. In addition to providing criteria for qualitative determination of whether a sample has undergone extensive periods of burial below the zone of cosmic ray penetration, ^{26}Al:^{10}Be ratios may be used to determine the timing of events that resulted in such burial (e.g., [14]).

3.4. Bioturbation

Bioturbation can have significant impacts on depth distributions of cosmogenic nuclides, bringing material with a near-surface exposure history to greater depth. It does not affect surface concentrations in system at steady state with respect to loss by erosion, but it increases both the time required to reach steady state and the soil column inventory at steady state. Details of these relationships are derived elsewhere [10]. Profiles of ^{10}Be in soils affected by bioturbation are generally constant in the bioturbated zone and have rather sharp decreases in concentration at the base of the reworked zone, returning to an undisturbed exponential profile.

Field studies have demonstrated the response of soil profiles to burial and bioturbation. Profiles of ^{10}Be in quartz sand extracted from soils were determined for the soil sequence at the Goyoum catena in east central Cameroon (5°14′N 13°18′E, 600–700 m) [5]. This site has undergone detailed studies of tropical weathering processes [2,24,25]. A series of sampling pits permit study of soil development at the summit, the slope and at the base of a plateau-like hill. The
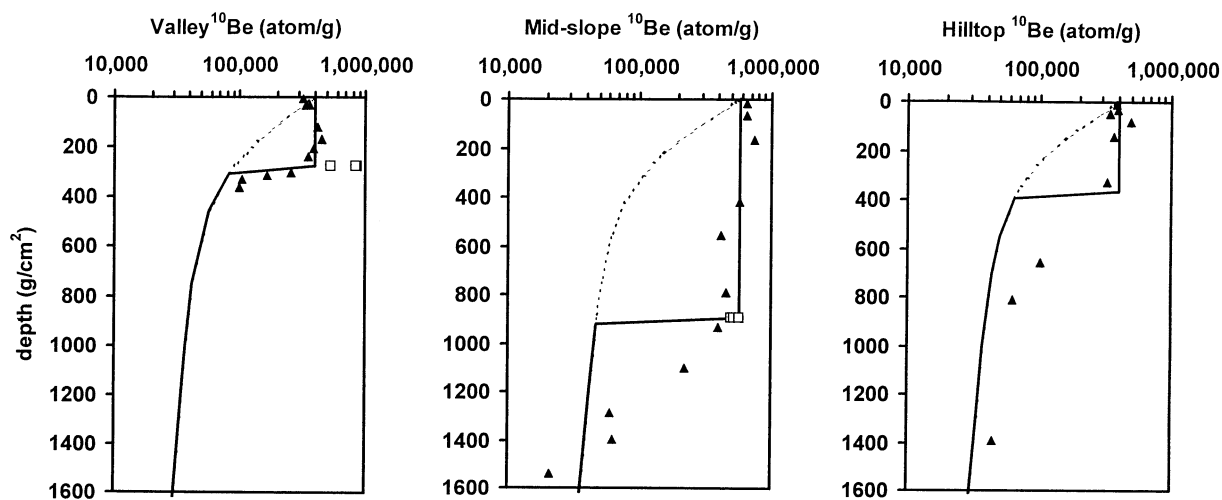
Fig. 6. Profiles of [10]Be in a series of soil pits (Goyoum, Cameroon) affected by bioturbation. The profiles were taken at the summit, slope and base of a hill. Theoretical profiles for non-bioturbated and bioturbated profiles at steady state are shown as dotted and solid lines. They were calculated using erosion rates that yield average [10]Be concentrations in the bioturbated layer. The measured profiles of [10]Be in quartz isolated from soils (filled symbols) are consistent with bioturbation to throughout the topsoil, to the depth of the underlying indurated nodular layer. Gravel-sized quartz present at this depth (open symbols) has higher [10]Be contents than observed within the soils, suggesting exposure closer to the surface. See text for further discussion.

Fig. 6. Courbes de [10]Be dans une série de puits pédologiques (Goyoum, Cameroun) affectés par la bioturbation. Les profils ont été prélevés au sommet, sur la pente et à la base de la colline. Les courbes théoriques pour des profils non bioturbés et bioturbés à l'équilibre sont représentées respectivement par les lignes en pointillé et des lignes continues. Elles sont calculées en utilisant des taux d'érosion qui fournissent des concentrations moyennes de [10]Be dans l'horizon bioturbé. Les courbes mesurées pour [10]Be dans des grains de quartz isolés de sols (symboles pleins) sont cohérentes avec la bioturbation vers (et au sein de) l'horizon supérieur et vers la profondeur de l'horizon nodulaire induré sous-jacent. Le quartz, à la granulométrie de gravier, présent à cette profondeur (symboles ouverts) a des teneurs en [10]Be plus élevées que celles observées au sein des sols, ce qui fait supposer une exposition plus proche de la surface. Voir le texte pour une discussion complémentaire.

upper soil horizon at these sites consists of a layer of relatively soft clayey topsoil, which extends to the depth of a nodular layer of indurated Fe-rich nodules and quartz cobbles and pebbles. Below this depth the soils are comprised of weathered saprolite in which the mineral texture of the parent gneissic bedrock is preserved.

Profiles of [10]Be are consistent with the role of bioturbation in these soils, but also indicate a possible role of burial of surficial material (Fig. 6). The essentially constant [10]Be in the upper soil indicates that homogenization by bioturbation occurs on timescales more rapid than [10]Be accumulation. The higher concentrations of [10]Be in the upper layer of the mid-slope profile, relative to the hilltop profile, may be the result of exposure while material is transported downslope by soil creep (see Section 3.5). The depth of homogenous [10]Be concentrations extends to the indurated nodular layer, below which [10]Be distributions revert toward simple exponential decreases. This confirms that

bioturbation can mix soils to depths of several meters in tropical environments. The transition toward the exponential decreases in [10]Be expected for undisturbed material occurs over a relatively broad depth range, particularly in the mid-slope profile. This could be the result of occasional penetration of bioturbation into the deeper soils or recent accumulation of surface soils that buried materials with an imprint of the near-surface [10]Be production by neutrons. The latter scenario is unlikely at hilltop sites, but is not inconsistent with episodes of erosion and burial due to alluvial processes at the base of the hill.

The quartz cobbles and pebbles at the base of the bioturbated layer in these profiles also provide evidence for exposure closer to the surface. In the profile at the base of the hill the [10]Be content of these pebbles is elevated relative to the overlying bioturbated layer, suggesting possible burial. Examination of the ratio of [26]Al:[10]Be in these samples also indicates burial [5], consistent with field observations indicating that this

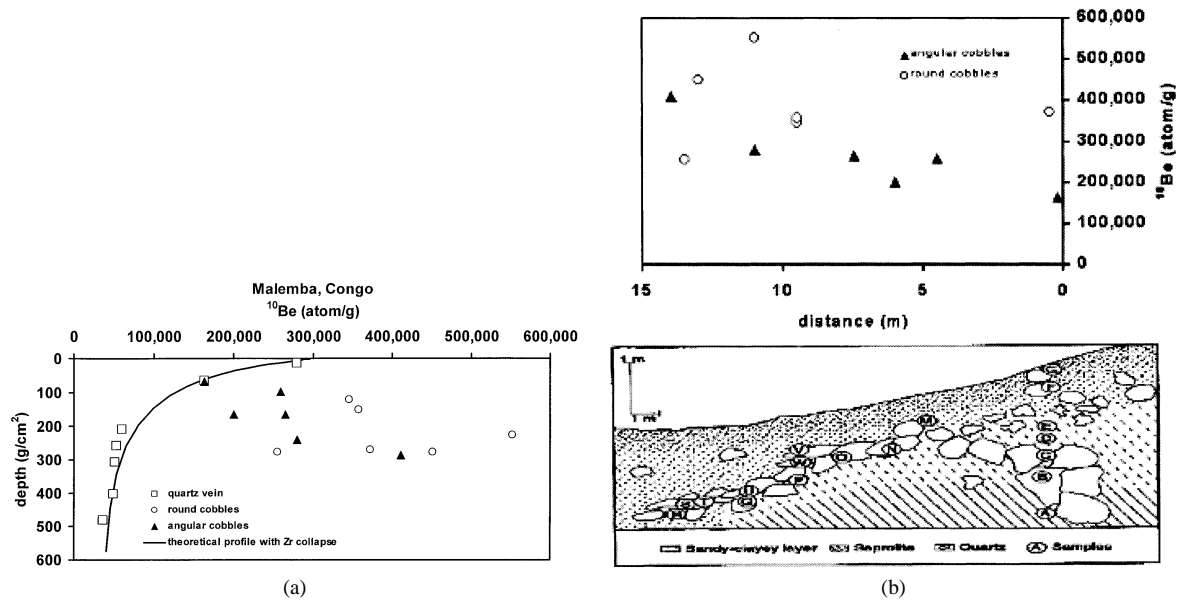(a)   (b)

Fig. 7. (**a**) Vertical distribution of [10]Be in a stoneline and vein quartz in soils exposed by a road cut (Malemba, Congo [3]). In contrast to the vein quartz, the stoneline clasts show no systematic variability with depth. In addition, their concentrations at any given depth are substantially higher than those of the vein quartz, indicating longer near-surface exposure. (**b**) Horizontal distribution of [10]Be in the Malemba stoneline. The rounded cobbles within the stoneline show no relationship with position within the stoneline, indicating an allochthonous origin. However, the angular clasts show a systematic increase in concentration with distance from the vein quartz outcropping at the hill's summit. This is consistent with an autochthonous origin consisting of dismantlement of the quartz vein followed by downslope movement. The increasing [10]Be content of the angular clasts may be used to estimate that downslope creep occurs at a rate of 50–90 m Myr^{-1}.

Fig. 7. (**a**) Distribution verticale de [10]Be dans une *stoneline* et un quartz de veine de sols mis à nu par une tranchée de route (Malemba, Congo [3]). Au contraire des grains de quartz de la veine, les fragments de *stoneline* ne montrent pas de variabilité systématique avec la profondeur. En outre, leurs concentrations, à n'importe quelle profondeur donnée, sont nettement plus fortes que celles de grains de quartz de la veine, indiquant une plus grande exposition près de la surface. (**b**) Distribution horizontale de [10]Be dans la *stoneline* de Malemba. Les fragments arrondis au sein de la *stoneline* ne montrent aucune relation avec leur position dans la *stoneline*, ce qui indique une origine allochtone. Cependant, les fragments anguleux montrent une augmentation systématique en concentration, au fur et à mesure que l'on s'écarte de l'affleurement de la veine quartzeuse, au sommet de la colline. Ceci est cohérent avec une origine autochtone, consistant en un démantèlement de la veine de quartz, suivi d'un mouvement vers le bas de pente. L'augmentation de la teneur en [10]Be des fragments anguleux peut être utilisée pour estimer qu'un fluage en bas de pente s'est produit à une vitesse de 50–90 m Ma^{-1}.

profile is part of an abandoned alluvial system. However, the [26]Al:[10]Be ratio in stoneline samples from the mid-slope profile also suggests burial. Burial of individual clasts does not necessarily require accumulation of material; larger clasts within a developing soil tend to be difficult for bioturbating organisms (e.g., worms, termites) to bring back to the surface.

3.5. Formation of 'stonelines' and horizontal displacement

Soil profiles in the humid tropics commonly include 'stonelines' – discrete horizons of quartz pebbles and cobbles (see [21] for a discussion). The processes leading to the formation of these features remain poorly understood. A major question to be addressed is whether stonelines result from in situ chemical weathering, are produced by large-scale erosive cycles and physical transport, and/or are formed by physical transport at the scale of the topographical unit.

These proposed mechanisms of stoneline formation will lead to distinct depth distributions of in situ-produced cosmogenic nuclides. The utility of cosmogenic nuclides in identifying the origin of stonelines and in quantifying the processes leading to their formation can be illustrated by field examples. At the hill in Malemba, Congo (described in Section 3.2 and shown in Fig. 7) a stoneline extends downslope at

the base of a sandy–clayey topsoil. This stoneline is composed of both rounded quartz cobbles and angular quartz clasts. In contrast to the relict quartz vein near the hill's summit, the stoneline material shows no systematic variability in concentration with subsurface depth, and has concentrations far in excess of those observed in the quartz vein (Fig. 7a). When examined as a function of horizontal distance downslope the rounded cobbles still show no systematic variation, but the angular cobbles have [10]Be concentrations that increase nearly linearly with downslope distance (Fig. 7b). These observations lead to three qualitative conclusions regarding the formation of this stoneline: (1) clasts within the stoneline has a history of exposure closer to the surface than its present positions; (2) the rounded cobbles are likely to have been exposed elsewhere before deposition and to have an allochthonous origin; (3) the systematic variability in [10]Be concentrations in the angular cobbles indicates that they are autochthonous, suggesting that they may result from dismantling and downslope transport (pre-
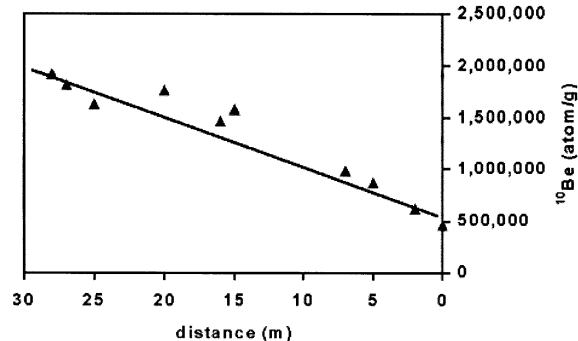

Fig. 8. Horizontal distribution of [10]Be in a stoneline from Itaberaba, Brazil [4]. The systematic increase in [10]Be concentration with horizontal distance from a dismantled quartz vein indicates that this vein feeds quartz to the stoneline, which then is subject to downslope creep. Depending upon the assumptions made about depth histories of clasts within the stoneline, [10]Be distributions indicate a creep rate of approximately 65 m Myr[−1].

Fig. 8. Distribution horizontale de [10]Be dans une *stoneline* d'Itaberaba (Brésil) [4]. L'augmentation systématique de la concentration en [10]Be au fur et à mesure que l'on s'écarte horizontalement de la veine de quartz démantelée indique que cette veine nourrit en quartz la *stoneline*, qui est ensuite sujette à un fluage de bas de pente. Si l'on se base sur les hypothèses des histoires en profondeur des fragments de *stoneline* au sein de celle-ci, les répartitions de [10]Be indiquent un taux de fluage d'approximativement 65 m Ma[−1].

sumably through soil creep) of the outcropping quartz vein (Fig. 7b).

Distributions of cosmogenic nuclides in stoneline clasts also provide a means for quantifying rates of horizontal movement. As stoneline clasts move downslope from an outcropping quartz vein, they undergo further exposure to cosmic rays, and accumulate additional cosmogenic nuclides. Evaluation of the angular clasts in the stoneline at Malemba indicates model creep rates of 50 and 90 m Myr[−1]. These results are from calculations that assume, respectively, either that each clast remained at a constant depth as it moved downslope or that the subsurface form of the stoneline was constant over time such that each clast moved to progressively greater depths as it moved downslope [3]. If stoneline clasts were closer to the surface than the present stoneline depth, the model rate of downslope movement would be more rapid. This approach has been used in examining stoneline development at other sites, notably at Itaberaba, Brazil, where a very clear increase in concentration with distance from an outcropping quartz vein corresponds to a rate of horizontal movement of ~ 65 m Myr[−1] [4] (Fig. 8).

4. Quantification of basin-scale denudation

Erosion rates determined for discrete bedrock outcrops may be applied to broader areas in cases where there is little spatial variability in erosional conditions (see Section 3.1). However, cosmogenic nuclide accumulation can also be employed for estimating of long-term denudation rates on scales of drainage basins. This is possible because in many cases the cosmogenic nuclide content of sediment discharged by a river represents the average concentration–weighted for area and denudation rate of the various erosional environments present – for the basin as a whole [10,15]. Under such conditions, the following expression (Eq. (3)) may be employed to relate the long-term mean denudation rate of the basin to the measured average concentration [10]Be:

$$\bar{\varepsilon} = \frac{\overline{P}L}{\overline{N}}. \tag{3}$$

Here $\overline{P}$ represents the average production rate (at g[−1] yr^{−1}), weighted according the hypsometric curve

of the basin; $\bar{\varepsilon}$ is the basin-side average denudation rate ($g\,cm^{-2}\,yr^{-1}$); L is the effective attenuation length of cosmic rays penetrating rock or soil ($155\,g\,cm^{-2}$; see Section 3.1). Use of this simple exponential, required for this averaging approach, can induce small systematic errors in calculated erosion rates (Fig. 4). This approach complements drainage-basin mass balance estimates of denudation [22], providing a long-term context in which to consider modern erosion rates. The highly episodic nature of fluvial transport makes it instructive to consider denudation on multiple timescales. Furthermore, anthropogenic disturbances can increase physical erosion rates by orders of magnitude, precluding the use of mass balance for direct estimation of long-term denudation rates [30].

A number of studies have compared erosion rates induced from [10]Be in sediments with results from other methods. Comparisons with recent river basin mass balances have demonstrated that recent estimates can overestimate long-term (10^4 to 10^5 yr) rates in basins where major storms occurred during the period of the mass balance study [10] or where deforestation and conversion to agriculture have affected the basin [11]. In contrast, other studies have shown that long-term denudation rates can exceed modern rates at sites affected by rare catastrophic mass wasting events [18], or enhanced glacial erosion [28,29]. On the other hand, consistency between erosion rates based on cosmogenic nuclides in river sediments and 10^7-year average sediment removal rates based on fission track analyses has been used to argue for long-term geomorphic stability [1,23].

The roles of tectonics and climate in determining rates of chemical weathering and physical erosion have also been examined in studies that use [10]Be in riverine sediment [26,27]. The assumption of immobility of Zr during chemical weathering, in conjunction with [10]Be based river basin total erosion rates permitted separation of the effects of chemical and physical weathering in a number of catchments spanning a wide range of erosion rates and climates in the western United States. If Zr is slightly mobile, rather than immobile, the resultant weathering rates will underestimate chemical weathering. Nevertheless, these studies found that chemical weathering rates correlate strongly with physical erosion rates, but that these rates correlate only weakly with climate, implying

that climate only weakly regulates non-glacial erosion rates in mountainous granitic terrain.

5. Summary and conclusions

We have much to learn about material transfers at the Earth's surface; cosmogenic nuclides are providing new approaches to quantifying these processes. Recent studies have improved our understanding of production systematics of in situ produced cosmogenic nuclides. In particular, examination of the depth variability of their production has demonstrated the relative roles of neutrons, fast muons and stopping muons in [10]Be production. This permits more detailed application of depth profiles of this nuclide to evaluate a range of processes including collapse, erosion, burial, bioturbation, and creep, as well as providing a qualitative basis for distinguishing allochthonous from autochthonous materials. In addition, these nuclides can provide quantitative information on rates of erosion on scales of landforms and drainage basins. These studies can be used to compare modern erosion rates with longer-term values, and have been used in examining the interplay among tectonics, climate and weathering.

References

[1] P.R. Bierman, M. Caffee, Steady state rates of rock surface erosion and sediment production across the hyperarid Namib desert and the Namibian escarpment, southern Africa, Am. J. Sci. 301 (2001) 326–358.

[2] M. Boudeulle, J.P. Muller, Structural characteristics of hematite and goethite and their relationships with kaolinite in a laterite from Cameroon; a TEM study, Bull. Mineral. 111 (1988) 149–166.

[3] R. Braucher, F. Colin, E.T. Brown, D.L. Bourlès, O. Bamba, G.M. Raisbeck, F. Yiou, J.M. Koud, African laterite dynamics using in situ-produced [10]Be, Geochim. Cosmochim. Acta 62 (1998) 1501–1507.

[4] R. Braucher, D. Bourlès, F. Colin, E.T. Brown, B. Boulangé, Brazilian laterite dynamics using in situ-produced ^{10}Be, Earth Planet. Sci. Lett. 163 (1998) 197–205.

[5] R. Braucher, D. Bourlès, E.T. Brown, F. Colin, J.-P. Muller, J.-J. Braun, M. Delaune, A. Edou Minko, C. Lescouet, G.M. Raisbeck, F. Yiou, Application of in situ-produced cosmogenic ^{10}Be and ^{26}Al to the study of lateritic soil development in tropical forest: theory and examples from Cameroon and Gabon, Chem. Geol. 170 (2000) 95–111.

[6] R. Braucher, E.T. Brown, D.L. Bourlès, F. Colin, In situ-produced ^{10}Be measurements at great depths: Implications for production rates by fast muons, Earth Planet. Sci. Lett. 211 (2003) 251–258.

[7] E.T. Brown, R.F. Stallard, G.M. Raisbeck, F. Yiou, Determination of the denudation rate of Mount Roraima, Venezuela using cosmogenic ^{10}Be and ^{26}Al, EOS 73 (1992) 170.

[8] E.T. Brown, D.L. Bourlès, F. Colin, Z. Sanfo, G.M. Raisbeck, F. Yiou, The development of iron crust lateritic systems in Burkina Faso, West Africa, examined with in situ-produced cosmogenic nuclides, Earth Planet. Sci. Lett. 124 (1994) 19–33.

[9] E.T. Brown, D.L. Bourlès, F. Colin, G.M. Raisbeck, F. Yiou, S. Desgarceaux, Evidence for muon-induced in situ production of ^{10}Be in near surface rocks from the Congo, Geophys. Res. Lett. 22 (1995) 703–706.

[10] E.T. Brown, R.F. Stallard, M.C. Larsen, G.M. Raisbeck, F. Yiou, Denudation rates determined from the accumulation of in situ produced ^{10}Be in the Luquillo Experimental Forest, Puerto Rico, Earth Planet. Sci. Lett. 129 (1995) 193–202.

[11] E.T. Brown, R.F. Stallard, M.C. Larsen, D.L. Bourlès, G.M. Raisbeck, F. Yiou, Determination of predevelopment denudation rates of an agricultural watershed (Cayaguas River, Puerto Rico) using in-situ-produced ^{10}Be in river-borne quartz, Earth Planet. Sci. Lett. 160 (1998) 723–728.

[12] T.E. Cerling, H. Craig, Geomorphology and in-situ cosmogenic isotopes, Annu. Rev. Earth Planet. Sci. 22 (1994) 273–317.

[13] F. Colin, C. Alarçon, P. Vieillard, Zircon: an immobile index in soils?, Chem. Geol. 107 (1993) 273–276.

[14] D.E. Granger, P.F. Muzikar, Dating sediment burial with in situ-produced cosmogenic nuclides: theory, techniques, and limitations, Earth Planet. Sci. Lett. 188 (2001) 269–281.

[15] D.E. Granger, J.W. Kirchner, R. Finkel, Spatially averaged long-term erosion rates measured from in situ-produced cosmogenic nuclides in alluvial sediment, J. Geol. 104 (1996) 249–257.

[16] B. Heisinger, D. Lal, A.J.T. Jull, P. Kubik, S. Ivy-Ochs, S. Neumaier, K. Knie, V. Lazarev, E. Nolte, Production of selected cosmogenic radionuclides by muons. 1. Fast muons, Earth Planet. Sci. Lett. 200 (2002) 345–355.

[17] B. Heisinger, D. Lal, A.J.T. Jull, P. Kubik, S. Ivy-Ochs, K. Knie, E. Nolte, Production of selected cosmogenic radionuclides by muons. 2. Capture of negative muons, Earth Planet. Sci. Lett. 200 (2002) 357–369.

[18] J.W. Kirchner, R.C. Finkel, C.S. Riebe, D.E. Granger, J.L. Clayton, J.G. King, W.F. Megahan, Mountain erosion over 10 yr, 10 kyr, and 10 Myr time scales, Geology 29 (2001) 591–594.

[19] M.D. Kurz, E.J. Brook, Surface exposure dating with cosmogenic nuclides, in: C. Beck (Ed.), Dating in a Surface Context, University of New Mexico Press, Albuquerque, NM, USA, 1994.

[20] D. Lal, K. Nishiizumi, J. Arnold, In situ cosmogenic ^{3}H, ^{14}C and ^{10}Be for determining the net accumulation and ablation rates of ice sheets, J. Geophys. Res. 92 (1987) 4947–4952.

[21] P. Lecomte, Stoneline profiles: importance in geochemical exploration, J. Geochem. Explor. 30 (1988) 35–61.

[22] G.E. Likens, F.H. Bormann, R.S. Pierce, J.S. Eaton, N.M. Johnson, Biogeochemistry of a Forested Ecosystem, Springer-Verlag, New York, 1977, 146 p.

[23] A. Matmon, P.R. Bierman, J. Larsen, S. Southworth, M. Pavich, M. Caffee, Temporally and spatially uniform rates of erosion in the southern Appalachian Great Smoky Mountains, Geology 31 (2003) 155–158.

[24] J.-P. Muller, Oxi-hydroxides geneses and their interrelationships with kaolinite in a laterite; petrological implications, Chem. Geol. 84 (1990) 314–315.

[25] J.-P. Muller, G. Calas, Tracing kaolinites through their defect centers; kaolinite paragenesis in a laterite (Cameroon), Econ. Geol. 84 (1989) 694–707.

[26] C.S. Riebe, J.W. Kirchner, D.E. Granger, R.C. Finkel, Minimal climatic control on erosion rates in the Sierra Nevada, California, Geology 29 (2001) 447–450.

[27] C.S. Riebe, J.W. Kirchner, D.E. Granger, R.C. Finkel, Strong tectonic and weak climatic control of long-term chemical weathering rates, Geology 29 (2001) 511–514.

[28] M. Schaller, F. von Blanckenburg, N. Hovius, P.W. Kubik, Large-scale erosion rates from in situ-produced cosmogenic nuclides in European river sediments, Earth Planet. Sci. Lett. 188 (2001) 441–458.

[29] M. Schaller, F. von Blanckenburg, A. Veldkamp, L.A. Tebbens, N. Hovius, P.W. Kubik, A 30 000-yr record of erosion rates from cosmogenic ^{10}Be in Middle European river terraces, Earth Planet. Sci. Lett. 204 (2002) 307–320.

[30] R.F. Stallard, Relating chemical and physical erosion, Rev. Mineral. 31 (1995) 543–564.

[31] M.G. Zreda, F.M. Phillips, Cosmogenic nuclide buildup in surficial materials, in: J.S. Noller, J.M. Sowers, W.R. Lettis (Eds.), Quaternary Geochronology: Methods and Applications, Am. Geophys. Union, Washington DC, 2000, pp. 61–76.